J|A|C|S
ARTICLES

Published on Web 11/08/2008

The Influence of Poly(3-hexylthiophene) Regioregularity on Fullerene-Composite Solar Cell Performance

Claire H. Woo,[†,‡] Barry C. Thompson,[§] Bumjoon J. Kim,[‡,§] Michael F. Toney,[||] and Jean M. J. Fréchet*[,†,‡,§]

Department of Chemical Engineering, University of California, Berkeley, California 94720, Materials Sciences Division, Lawrence Berkeley National Laboratory, Berkeley, California 94720, Department of Chemistry, University of California, Berkeley, California 94720, and Stanford Synchrotron Radiation Laboratory, Menlo Park, California 94205

Received August 15, 2008; E-mail: frechet@berkeley.edu

Abstract: A comparison of three samples of poly(3-hexylthiophene) having regioregularities of 86, 90, and 96% is used to elucidate the effect of regioregularity on polymer−fullerene-composite solar cell performance. It is observed that polymer samples with lower regioregularity are capable of generating fullerene composites that exhibit superior thermal stability. The enhanced thermal stability of the composites is attributed to a lower driving force for polymer crystallization in the less regioregular polymer samples, which is supported with two-dimensional grazing incidence X-ray scattering and differential scanning calorimetry measurements. Furthermore, it is demonstrated that all three polymer samples are capable of generating solar cells with equivalent peak efficiencies of ∼4% in blends with [6,6]-phenyl-C_{61}-butyric acid methyl ester. While it may be non-intuitive that polymers with lower regioregularity can exhibit higher efficiencies, it is observed that the charge-carrier mobility of the three polymers is on the same order of magnitude (10^{-4} cm^2 V^{-1} s^{-1}) when measured from the space-charge-limited current, suggesting that highly regioregular and crystalline polythiophenes are not required in order to effectively transport charges in polymer solar cells. Overall, these results suggest a design principle for semicrystalline conjugated polymers in fullerene-composite solar cells in which crystallization-driven phase separation can be dramatically suppressed via the introduction of a controlled amount of disorder into the polymer backbone.

Introduction

Polymer−fullerene-composite solar cells (bulk heterojunction solar cells) define the state of the art in organic photovoltaics, with reported efficiencies as high as ∼5%.[1−4] The applicability of solution processing techniques under ambient temperature and pressure makes this class of solar cell especially attractive in the search for low-cost methods of harvesting solar energy.[5] While several new high-performing polymer−fullerene combinations have recently been reported,[6,7] the combination of poly(3-hexylthiophene) (P3HT) and [6,6]-phenyl-C_{61}-butyric acid methyl ester (PCBM) still gives a power conversion efficiency (PCE) among the highest reported.[3,4] This is despite the nonideal band gap of P3HT (∼1.9 eV) that prevents effective overlap with the solar spectrum, which peaks at ∼1.8 eV. Numerous polymers have been synthesized that exhibit more optimal band gaps and blanket the solar spectrum more effectively,[8,9] but almost none have exceeded the performance of P3HT.[6] This can be attributed to an incomplete set of design principles for an ideal donor polymer for fullerene-composite solar cells, which currently is exclusively based on the electronic interaction of the polymer and the fullerene[1,8,10] and ignores the features of the polymer primary structure that influence the formation of active layers with bicontinuous and thermally stable morphologies.

Toward this end, P3HT is targeted as a model semicrystalline polymer from which general relationships between primary structure and function can be extrapolated. The key variables of polymer primary structure in P3HT are molecular weight, polydispersity, and regioregularity (RR). In each case, efforts to elucidate the effect of each individual variable on photovoltaic performance have been pursued.[11−14] The developing picture

[†] Department of Chemical Engineering, University of California.
[‡] Lawrence Berkeley National Laboratory.
[§] Department of Chemistry, University of California.
[||] Stanford Synchrotron Radiation Laboratory.

(1) Thompson, B. C.; Fréchet, J. M. J. *Angew. Chem., Int. Ed.* **2008**, *47*, 58–77.
(2) Gunes, S.; Neugebauer, H.; Sariciftci, N. S. *Chem. Rev.* **2007**, *107*, 1324–1338.
(3) Ma, W.; Yang, C.; Gong, X.; Lee, K.; Heeger, A. J. *Adv. Funct. Mater.* **2005**, *15*, 1617–1622.
(4) Li, G.; Shrotriya, V.; Huang, J.; Yao, Y.; Moriarty, T.; Emery, K.; Yang, Y. *Nat. Mater.* **2005**, *4*, 864–868.
(5) Hoth, C. N.; Choulis, S. A.; Schilinsky, P.; Brabec, C. J. *Adv. Mater.* **2007**, *19*, 3973–3978.
(6) Peet, J.; Kim, J. Y.; Coates, N. E.; Ma, W. L.; Moses, D.; Heeger, A. J.; Bazan, G. C. *Nat. Mater.* **2007**, *6*, 497–500.
(7) Wienk, M. M.; Turbiez, M.; Gilot, J.; Janssen, R. A. J. *Adv. Mater.* **2008**, *20*, 2556–2560.
(8) Thompson, B. C.; Kim, Y.; McCarley, T. D.; Reynolds, J. R. *J. Am. Chem. Soc.* **2006**, *128*, 12714–12725.
(9) Blouin, N.; Michaud, A.; Gendron, D.; Wakim, S.; Blair, E.; Neagu-Plesu, R.; Belletete, M.; Durocher, G.; Tao, Y.; Leclerc, M. *J. Am. Chem. Soc.* **2008**, *130*, 732–742.
(10) Scharber, M.; Mühlbacher, D.; Koppe, M.; Denk, P.; Waldauf, C.; Heeger, A. J.; Brabec, C. J. *Adv. Mater.* **2006**, *18*, 789–794.
(11) Schilinsky, P.; Asawapirom, U.; Scherf, U.; Biele, M.; Brabec, C. J. *Chem. Mater.* **2005**, *17*, 2175–2180.

 10.1021/ja806493n CCC: $40.75

suggests that high molecular weight (M_n > 20 000 g/mol), broad polydispersity (PDI), and high RR (>95%) are optimal for solar cell performance, as can be supported via both observed increases in efficiency when these parameters are satisfied and extrapolation from structure−function relationships observed in pristine samples of P3HT.[15−18] However, all of these conclusions come with caveats. First, while high molecular weight has been shown to improve charge-carrier mobility and optical properties in pristine, high-RR P3HT films, solar cells using P3HT of significantly lower molecular weight (~11 000 g/mol) have been reported to give efficiencies over 4% under optimized processing conditions.[13] Second, a systematic study of the effect of the polydispersity of P3HT has not been reported, although it does appear that a broad mix of high- and low-molecular-weight P3HT in a given sample improves the performance of P3HT−PCBM-composite solar cells.[12] Finally, the only systematic study of the effect of P3HT RR, which points to increasing efficiency with increasing RR, is based on a comparison of devices for which the processing conditions had not been optimized.[13] In view of the enormous effects that are known for variations in solvent,[19,20] blend ratio,[21,22] spin speed,[20,23] annealing conditions,[4,24,25] and electrode structure,[26,27] such unoptimized results are not necessarily definitive. The study by Kim et al.[13] examined the range of RR from 90.7−95.4% and showed that samples in the 90.7−93.0% range have efficiencies of under 2%, which is lower than the 4−5% efficiencies reported in the literature using P3HT from Rieke Metals (RR ~92%).[3,28] It has also been shown that a copolymer analogue of P3HT with an effective RR of 91% was capable of producing solar cells with a PCE of 4.5%.[28] It is therefore clear that the definitive effect of P3HT RR on fullerene-composite solar cells is not yet known. In this work, we examined three samples of P3HT having similar molecular weight and PDI that were polymerized by the same polymerization method but in which the RR varied from 86 to 96%. This RR range was selected in order to look at a high-RR P3HT (96%), a sample with a RR similar to that of Rieke P3HT (90%), and a sample with a significantly lower RR than has been reported in most P3HT−PCBM solar cells (86%). The lowest RR value was attained via a copolymerization of 2-bromo-3-hexylthiophene and 5-bromo-3,3′-dihexyl-2,2′-bithiophene (see the Supporting Information). Solar cell performance and long-term thermal stability were examined within the context of variations in the fundamental properties of the polymers induced via changes to the primary structure in the form of non-head-to-tail "defect" linkages.

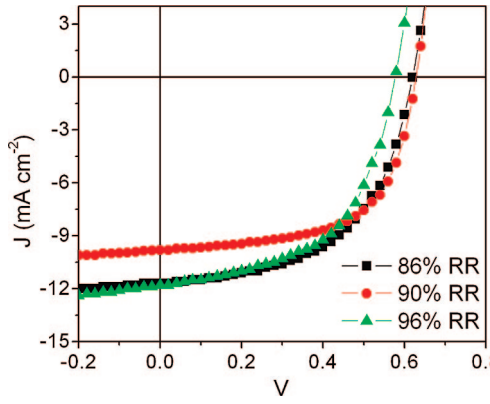

Figure 1. *I*−*V* characteristics of optimized devices made from 86, 90, and 96% RR P3HT blended with PCBM at a 55:45 weight ratio. For 86% RR (■): V_{oc} = 0.62 V, J_{sc} = −11.7 mA/cm^2, FF = 0.54, PCE = 3.9%. For 90% RR (●): V_{oc} = 0.63 V, J_{sc} = −9.8 mA/cm^2, FF = 0.61, PCE = 3.8%. For 96% RR (▲): V_{oc} = 0.58 V, J_{sc} = −11.8 mA/cm^2, FF = 0.55, PCE = 3.8%.

Results

Solar Cell Performance. The performance of each polymer was independently optimized according to annealing conditions while the polymer−PCBM blend ratio was kept constant at 55:45 by weight and the devices all had similar thicknesses (~100 nm). Figure 1 shows the *I*−*V* characteristics of the most efficient P3HT−PCBM bulk heterojunction (BHJ) devices made from 86, 90, and 96% RR P3HT, which achieved peak PCEs of 3.9, 3.8, and 3.8%, respectively, under AM 1.5G illumination with an intensity of 100 mW cm^{-2}. First, it is noteworthy that P3HT with RR as low as 86% can still achieve close to 4% PCE. A second observation is that the optimized annealing time was different for the three polymers. At an annealing temperature of 150 °C, the device with 96% RR P3HT required the shortest annealing time (30 min) to reach the highest efficiency, whereas the devices with 90 and 86% RR P3HT required longer annealing times (60 and 120 min, respectively). The slightly lower J_{sc} in the device with 90% RR may be due to the lower molecular weight of the polymer, which may influence the parameters of device performance,[11,12] but the high fill factor (FF) of this device compensates for this reduction in current, allowing it to attain an efficiency comparable to those of the devices made from 86 and 96% RR P3HT. In addition, there appears to be a trend in which higher RR gives a lower V_{oc}. On average, 96% RR P3HT devices had a V_{oc} of 0.58 V whereas 86% RR devices had a V_{oc} of 0.62V.

The thermal stabilities of the photovoltaic devices were also examined, and Figure 2 shows for each RR level the evolution

(12) Ma, M.; Kim, J. Y.; Lee, K.; Heeger, A. J. *Macromol. Rapid Commun.* **2007**, *28*, 1776–1780.
(13) Kim, Y.; Cook, S.; Tuladhar, S. M.; Choulis, S. A.; Nelson, J.; Durrant, J. R.; Bradley, D. D. C.; Giles, M.; McCullough, I.; Ha, C. S.; Ree, M. *Nat. Mater.* **2006**, *5*, 197–203.
(14) Urien, M.; Bailly, L.; Vignau, L.; Cloutet, E.; de Cuendias, A.; Wantz, G.; Cramail, H.; Hirsch, L.; Parneix, J. *Polym. Int.* **2008**, *57*, 764–769.
(15) Kline, R. J.; McGehee, M. D.; Kadnikova, E. N.; Liu, J.; Fréchet, J. M. J.; Toney, M. F. *Macromolecules* **2005**, *38*, 3312–3319.
(16) Zen, A.; Pflaum, J.; Hirschmann, S.; Zhuang, W.; Jaiser, F.; Asawapirom, U.; Rabe, J. P.; Scherf, U.; Neher, D. *Adv. Funct. Mater.* **2004**, *14*, 757–764.
(17) Sirringhaus, H.; Brown, P. J.; Friend, R. H.; Nielsen, M. M.; Bechgaard, K.; Langeveld-Voss, B. M. W.; Spiering, A. J. H.; Janssen, R. A. J.; Meijer, E. W.; Herwig, P.; de Leeuw, D. M. *Nature* **1999**, *401*, 685–688.
(18) Barta, P.; Cacialli, F.; Friend, R. H.; Salaneck, W. R.; Zagorska, M.; Prori, A. *Synth. Met.* **1999**, *101*, 296–297.
(19) Kim, Y.; Choulis, S. A.; Nelson, J.; Bradley, D. D. C.; Cook, S.; Durrant, J. R. *Appl. Phys. Lett.* **2005**, *86*, 063502.
(20) Chu, C.-W.; Yang, H.; Hou, W. J.; Huang, J.; Li, G.; Yang, Y. *Appl. Phys. Lett.* **2008**, *92*, 103306.
(21) Nakamura, J.; Murata, K.; Takahashi, K. *Appl. Phys. Lett.* **2005**, *87*, 132105.
(22) Chirvase, D.; Parisi, J.; Hummelen, J. C.; Dyakonov, V. *Nanotechnology* **2004**, *15*, 1317–1323.
(23) Shrotriya, V.; Yao, Y.; Li, G.; Yang, Y. *Appl. Phys. Lett.* **2006**, *89*, 063505.
(24) Reyes-Reyes, M.; Kim, K.; Carroll, D. L. *Appl. Phys. Lett.* **2005**, *87*, 083506.
(25) Yang, X.; Loos, J.; Veenstra, S. C.; Verhees, W. J. H.; Wienk, M. M.; Kroon, J. M.; Michels, M. A. J.; Janssen, R. A. J. *Nano Lett.* **2005**, *5*, 579–583.
(26) Ko, C.-J.; Lim, Y.-K.; Chen, F.-C.; Chu, C.-W. *Appl. Phys. Lett.* **2007**, *90*, 063509.
(27) Kim, J. Y.; Kim, S. H.; Lee, H.-H.; Lee, K.; Ma, W.; Gong, X.; Heeger, A. J. *Adv. Mater.* **2006**, *18*, 572–576.
(28) Sivula, K.; Luscombe, C. K.; Thompson, B. C.; Fréchet, J. M. J. *J. Am. Chem. Soc.* **2006**, *128*, 13988–13989.

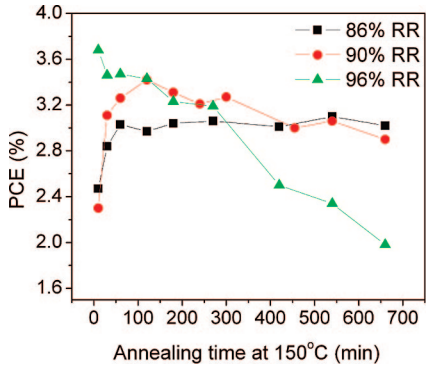

Figure 2. Average efficiencies of 86, 90, and 96% RR P3HT−PCBM BHJ devices annealed at 150 °C for different times. The efficiency of the 96% RR P3HT devices decreased drastically after 5 h of annealing, but the 90 and 86% RR devices maintained ∼3% efficiencies after 11 h of annealing.

of the average efficiency of eight P3HT−PCBM BHJ devices after thermal annealing at 150 °C for various times. The unannealed devices (not shown on figure) all had efficiencies of <1%. After 10 min of annealing, the 96% RR P3HT devices achieved their highest efficiencies, while the 90 and 86% RR P3HT devices required longer annealing times to achieve PCEs in excess of 3%. However, the trend was reversed for longer annealing times. Devices consisting of 96% RR P3HT decayed quickly to less than 2.5% PCE after 5 h of annealing, whereas devices with 86 and 90% RR P3HT were able to maintain ∼3% PCE after more than 10 h of annealing at 150 °C, which serves as an accelerated performance test.

Blend Morphology. Optical microscopy was used to provide a qualitative inspection of the P3HT−PCBM blend morphology. Figure 3 shows optical micrographs of P3HT samples with different RRs blended with PCBM at a 55:45 weight ratio and annealed at 150 °C for 3 h. As shown in Figure 3a, a blend of 86% RR P3HT with PCBM shows only a few small PCBM crystals; the blend of 90% RR P3HT with PCBM (Figure 3b) shows larger and denser PCBM crystals within an area of the same size, but there is still a considerable area of well-mixed blend where large PCBM crystals are absent. In contrast, the optical micrograph of a blend of 96% RR P3HT with PCBM (Figure 3c) shows many large needlelike PCBM crystals that are more than 100 μm in length. These optical micrographs show that the morphology resulting from highly RR P3HT blends with PCBM displays extreme phase segregation after thermal annealing, and this segregation can damage performance in a solar cell, since the effective area of the device decreases as aggregation of PCBM crystals takes up larger areas. The same trend in morphology was observed under scanning electron microscopy (see Figure S4 in the Supporting Information). Zooming in on the homogeneous parts of the films of the 86 and 96% RR P3HT−PCBM blend samples, one can see bicontinuous networks of P3HT and PCBM under transmission electron microscopy (see Figure S5 in the Supporting Information). Similar needlelike PCBM crystals in blend films with P3HT had been observed by others and were believed to be due to the fast diffusion of PCBM toward the PCBM crystals, whose growth rate depends on blend composition and annealing conditions.[29,30] Here we have shown that in addition to the

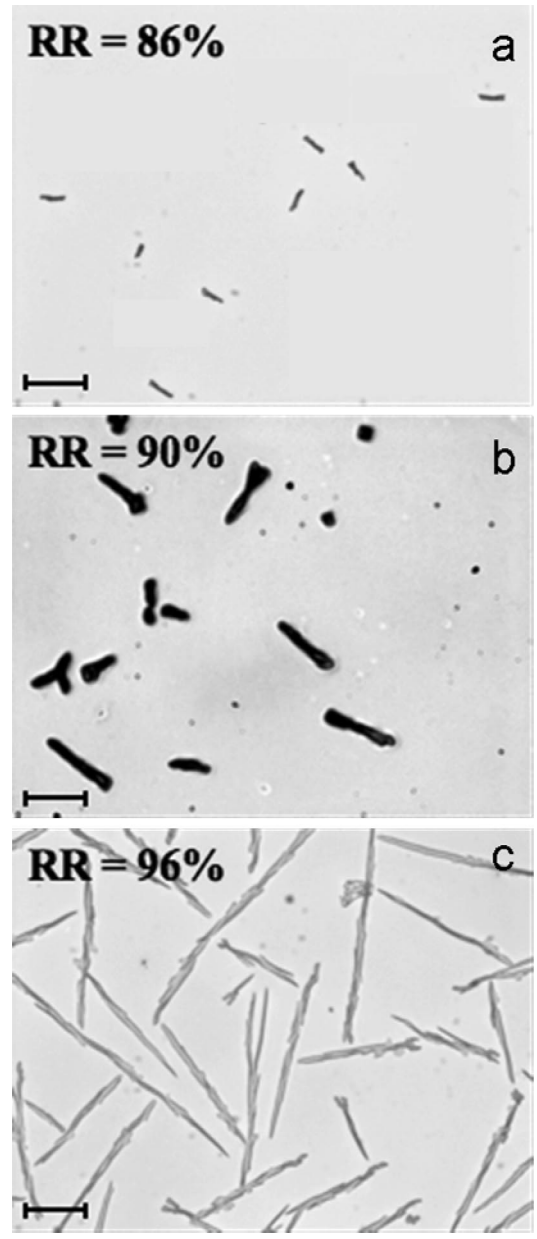

Figure 3. Optical microscopy images of (a) 86, (b) 90, and (c) 96% RR P3HT−PCBM blends at a 55:45 weight ratio after 3 h of annealing at 150 °C. Dark areas are PCBM-rich regions.[29,30] Scale bar = 50 μm.

processing conditions of the film, the chemical nature of the polymer significantly affects the extent of growth of these PCBM crystals during thermal annealing.

The blend morphology obtained from P3HT of different RR mixed with PCBM was probed by two-dimensional (2D) grazing-incidence X-ray scattering (GIXS) measurements. Figure 4 compares the GIXS patterns of 86, 90, and 96% RR P3HT blends with PCBM after 1 h of annealing at 150 °C. To produce identical surface conditions as samples for device measurement, a thin layer (20−30 nm) of PEDOT−PSS was spun onto silicon substrates and the P3HT−PCBM blend layer was subsequently spin-coated on top. The angle of incidence (∼0.1°) was carefully chosen to allow for complete penetration of the X-rays into the

(29) Swinnen, A.; Haeldermans, I.; Vande Ven, M.; D'Haen, J.; Vanhoyland, G.; Aresu, S.; D'Olieslaeger, M.; Manca, J. *Adv. Funct. Mater.* **2006**, *16*, 760–765.

(30) Campoy-Quiles, M.; Ferenzi, T.; Agosinelli, T.; Etchegoin, P. G.; Kim, Y.; Anthopoulos, T. D.; Stabrinou, P. N.; Bradley, D. C.; Nelson, J. *Nat. Mater.* **2008**, *7*, 158–164.

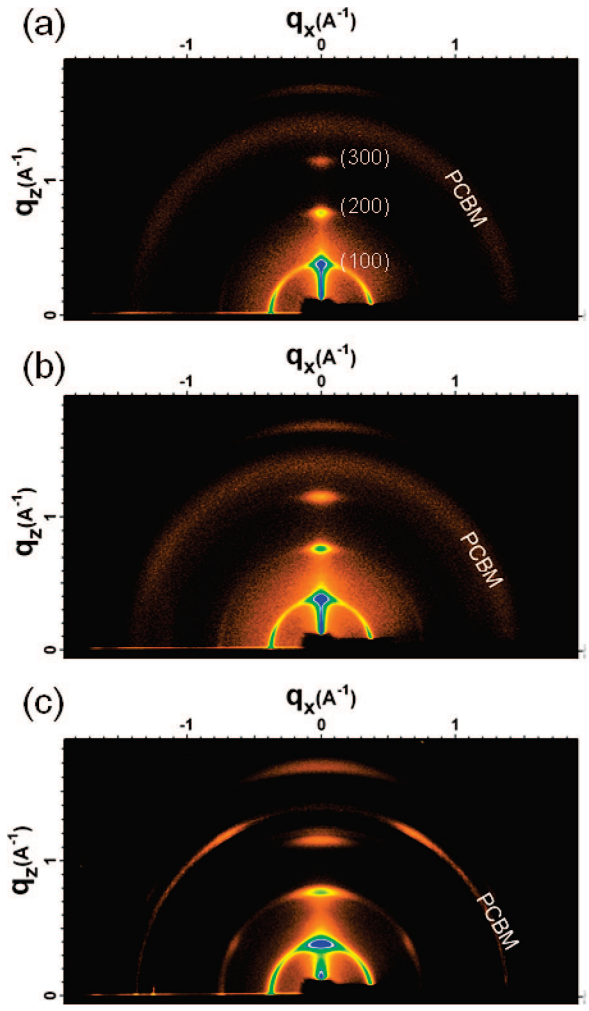

Figure 4. GIXS patterns of films of (a) 86, (b) 90, and (c) 96% RR P3HT−PCBM blends at a 55:45 weight ratio after 1 h of annealing at 150 °C. The vertical section at $q_x \approx 0$ is not the true specular direction (i.e., $q_x = 0$) but is tilted from this.

polymer film but only limited penetration into the substrate (to reduce the background). The 2D image map of a GIXS pattern can be divided into a component in the plane of the substrate (q_x) and a component perpendicular to the substrate (q_z), as shown in Figure 4. The (100), (200), and (300) diffraction peaks are strongest in the nominally out-of-plane direction but exhibit some arcing about this direction and some in-plane intensity (near $q_z \approx 0$). This shows that the P3HT−PCBM blend films have a well-organized structure in which most of the planar P3HT stacks are oriented along the perpendicular axis of the substrate. From the diffraction pattern, we extract a lamella spacing of 1.59 nm, which is consistent with that reported elsewhere.[17,31] The peak near the top of the images, at $q_z \approx 1.7$ Å^{-1} ($d = 0.38$ nm) is the (010) peak resulting from the $\pi-\pi$ stacking distance between P3HT chains.

The most distinct difference among the diffraction patterns from the three samples occurs at $q_z \approx 1.4$ Å^{-1} ($d = 0.46$ nm); this feature is due to PCBM, as determined by previous X-ray diffraction measurements.[31] The $q_z \approx 1.4$ Å^{-1} diffraction peak of PCBM is much sharper and more prominent in the 96% RR

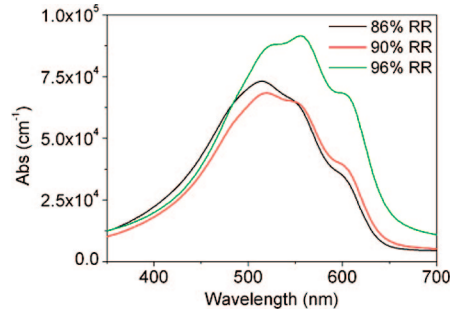

Figure 5. Absorption spectra of 86, 90, and 96% RR P3HT thin films annealed at 150 °C for 1 h.

P3HT blend film. In contrast, the PCBM peak is broad and diffuse in the two lower-RR samples. These GIXS images show that the PCBM is highly crystalline in the higher-RR−P3HT blend film, which is consistent with the larger extent of phase segregation observed using optical and electron microscopy.

Another noticeable and important difference among the samples is a difference in the extent of P3HT crystalline orientation. Specifically, the azimuthal angular width of the P3HT (100), (200), and (300) peaks in the 96% RR sample is much broader than for either the 90 or 86% RR sample. This indicates that the P3HT stacks are less well oriented in the 96% RR sample, i.e. more of the stacks are oriented away from the axis perpendicular to the substrate. This could be attributed to the presence of large PCBM crystallites in the 96% RR sample that force the P3HT stacks to orient away from the perpendicular plane and in more random directions.

Polymer Properties. The optical, electronic, and thermal properties of pristine polymers of different RRs were studied to investigate fundamental differences among these three polymers. The absorption spectra of thin films of P3HT of all three RR values are shown in Figure 5. The 96% RR P3HT has a higher optical density than the other two P3HT polymers. In addition, although all three polymers have similar absorption breadths, 86 and 90% RR P3HT have λ_{max} values of 514 and 519 nm, respectively, both of which are blue-shifted compared with the λ_{max} of 556 nm for the highly ordered 96% RR P3HT; the corresponding absorbances are 7.3×10^4, 6.8×10^4, and 9.2×10^4 cm^{-1}.

Besides absorption, charge-carrier mobility is of great importance in solar cells. The space-charge-limited current (SCLC) mobility measures the mobility in the direction perpendicular to the electrodes and thus is the most representative measurement of charge-carrier mobility for solar cells. For 86, 90, and 96% RR P3HT, the SCLC mobilities were measured to be 6.4×10^{-4}, 1.1×10^{-3}, and 1.1×10^{-3} cm^2 V^{-1} s^{-1}, respectively. These results are consistent with typical values for P3HT.[32] In addition, this type of behavior, where disrupting the order of the polymer does not affect the SCLC mobility, has been observed for another poly(alkylthiophene) system.[33] Although the SCLC mobility of the 86% RR P3HT is slightly lower than those of the other two P3HTs, the fact that the mobilities for all three polymers have the same order of magnitude indicates that reducing the RR within the range investigated does not significantly compromise the electronic properties of the polymer, as confirmed by the device results shown above.

(31) Vanlaeke, P.; Swinnen, A.; Haeldermans, I.; Vanhoyland, G.; Aernouts, T.; Cheyns, D.; Deibel, C.; D'Haen, J.; Heremans, P.; Poortmans, J.; Manca, J. V. *Sol. Energy Mater. Sol. Cells* **2006**, *90*, 2150–2158.
(32) Mihailetchi, V. D.; Xie, H.; de Boer, B.; Koster, L. J. A.; Blom, P. W. M. *Adv. Funct. Mater.* **2006**, *16*, 699–708.
(33) Thompson, B. C.; Kim, B. J.; Kavulak, D. F.; Sivula, K.; Mauldin, C.; Fréchet, J. M. J. *Macromolecules* **2007**, *40*, 7425–7428.

The GIXS results shown earlier suggest that there are differences in crystalline behavior (e.g., orientation) among the polymers of different RR and that this difference has a strong influence on blend morphology. To elucidate the quantitative difference in the crystallinity of the polymers, differential scanning calorimetry (DSC) measurements were performed. Degrees of crystallinity of the three polymer samples were calculated by comparing the heat of fusion for the particular polymer sample (ΔH_m) with that for an ideal crystal ($\Delta H_m^0 = 99$ J/g).[34−36] For 86, 90, and 96% RR P3HT, the degrees of crystallinity were measured to be 12, 15, and 21%, respectively, which are consistent with values reported by others for high-MW P3HT as measured by DSC.[34] These results show that crystallinity increases dramatically with RR. In addition, the DSC traces show increases in both the melting temperature (T_m) and the crystallization temperature (T_c) with increasing RR (see Figure S7 in the Supporting Information). The lower T_m values for the lower-RR samples indicate a more defective crystal structure. The two lower-RR P3HTs also showed a shoulder peak near the melting temperature, which could be characteristic of the existence of multiple crystal structures in the polymer sample.[34,37] The second smaller peak may also have arisen as a consequence of the melting of a less defective crystal generated via fast crystallization of the initial melt.

Discussion

It had been proposed that highly regioregular P3HT is preferred in solar cells since it has a stronger tendency to self-organize within the film, thus leading to higher crystallinity,[13] charge-carrier mobility,[17] and optical density.[13,18] Kim et al.[13] concluded that higher RR is necessary for achieving high-efficiency solar cells by comparing results for unoptimized devices. In their paper, they optimized the processing conditions only for the highest-RR P3HT devices and achieved 4.4% PCE. In contrast, our results show that with some optimization, similar peak performance (~4%) can be attained for 86, 90, and 96% RR P3HT. Although higher-RR P3HT may have a higher absorption coefficient, the difference between 86 and 96% RR polymers can easily be overcome by further optimization in the device fabrication process, such as longer annealing times to achieve the desired morphology. Measurements of SCLC mobilities have also demonstrated that the electronic properties of the polymer are maintained with decreasing RR within the range investigated. Moreover, devices made from lower-RR P3HT displayed superior thermal stability, suggesting that lower RR could be a better choice for P3HT−PCBM composite cells.

The difference in thermal stability of the different RR P3HT blends with PCBM correlates with the observed active-layer morphology as well as the degree of crystallinity data. First, optical microscopy results illustrate that the extent of phase separation is larger in the higher-RR P3HT−PCBM blend films after thermal annealing at 150 °C. Large PCBM crystals can be seen using optical and electron microscopy, and the PCBM crystalline peak in the GIXS pattern is much sharper and more distinct for the 96% RR P3HT blend sample. Second, DSC measurements confirm that higher-RR P3HT has a higher degree of crystallinity. These two observations suggest that the stronger driving force for crystallization of high-RR P3HT induces a larger extent of phase segregation (i.e., larger domains of pure phases) in a blend film with PCBM under a given thermal annealing condition, leading to faster deterioration of device performance. Interestingly, Kim et al.[13] also observed that a higher-RR polymer had a higher degree of crystallinity, and they claimed that this higher crystallinity was beneficial to device performance since it led to enhanced optical and electronic properties. In comparison, our results suggest a different picture in which the higher crystallinity of a higher-RR P3HT was a disadvantage, as it induces more phase segregation and leads to a less thermally stable blend morphology.

Strong correlations between crystallization and the resulting morphology in polymer blends have previously been established. In particular, crystallization of one or both blend components is known to induce phase segregation.[38−40] Thermal annealing causes crystallization of the highly ordered 96% RR P3HT and of PCBM in the active layer of the device, leading to extreme phase segregation of the two components that results in large crystallites of PCBM, thus reducing the interfacial area for charge transfer and leading to lower efficiencies. On the other hand, the weaker crystallization of lower-RR P3HT leads to weaker phase segregation in a blend film with PCBM, and it is shown that the larger amorphous content in the polymer inhibits large-scale PCBM crystallization; as a result, the desired interpenetrating network can withstand longer annealing treatment, thus improving the thermal stability of the device. In other words, although 86% RR P3HT may have slightly lower charge-carrier mobility and optical density, its lower degree of crystallinity gives it the advantage of limiting the extent of phase segregation with PCBM upon thermal annealing and maintaining the desired morphology for BHJ solar cells. While previous papers have focused on controlling PCBM diffusion by blend composition and annealing conditions,[29,30] our result is the first example of the use of varying degrees of polymer crystallinity to control phase segregation.

Of particular interest is the disruption in the orientation of P3HT crystals in the highly crystalline 96% RR polymer, which is indicated by the broadening of the crystalline peaks of P3HT shown in the GIXS patterns. This is possibly due to aggregation of PCBM, which can push P3HT crystallites away from the preferred orientation. Figure 6a is a schematic illustration of the twisting of P3HT stacks away from the perpendicular plane as a result of the presence of large PCBM crystals. In the high-RR P3HT sample, PCBM diffuses away from the highly crystalline polymer upon thermal annealing and aggregates together to a larger extent than in lower-RR P3HT, and these large crystallites can cause leaning of the P3HT stacks. As a result, the P3HT stacks become more randomly oriented, so fewer of them are perpendicular to the substrate, thus leading to broader crystalline P3HT peaks under X-ray scattering. In contrast, lower-RR P3HT−PCBM blends have a lesser extent of phase segregation, leading to fewer and smaller PCBM crystals and thus minimizing the randomization of the orientation of P3HT stacks, as illustrated schematically in Figure 6b and

(34) Zen, A.; Saphiannikova, M.; Neher, D.; Grenzer, J.; Grigorian, S.; Pietsch, U.; Asawapirom, U.; Janietz, S.; Scherf, U.; Lieberwirth, I.; Wegner, G. *Macromolecules* **2006**, *39*, 2162–2171.
(35) Malik, S.; Nandi, A. K. *J. Polym. Sci. B* **2002**, *40*, 2073–2085.
(36) Causin, V.; Marega, C.; Marigo, A.; Valentini, L.; Kenny, J. K. *Macromolecules* **2005**, *38*, 409–415.
(37) Swinnen, A.; Zhao, G.; Van Assche, D.; Vanderzande, D.; D'Olieslaeger, M.; Manca, J. V.; Van Mele, B. *Proc. SPIE−Int. Soc. Opt. Eng.* **2007**, *6656*, 665619.
(38) Defieuw, G.; Groeninckx, G.; Reynaers, H. *Polymer* **1989**, *30*, 2164–2169.
(39) Alamo, R. G.; London, J. D.; Mandelkern, L.; Stehling, F. C.; Wignall, G. D. *Macromolecules* **1994**, *27*, 411–417.
(40) Chiu, H.; Chen, H. L.; Lin, J. S. *Polymer* **2001**, *42*, 5769–5754.

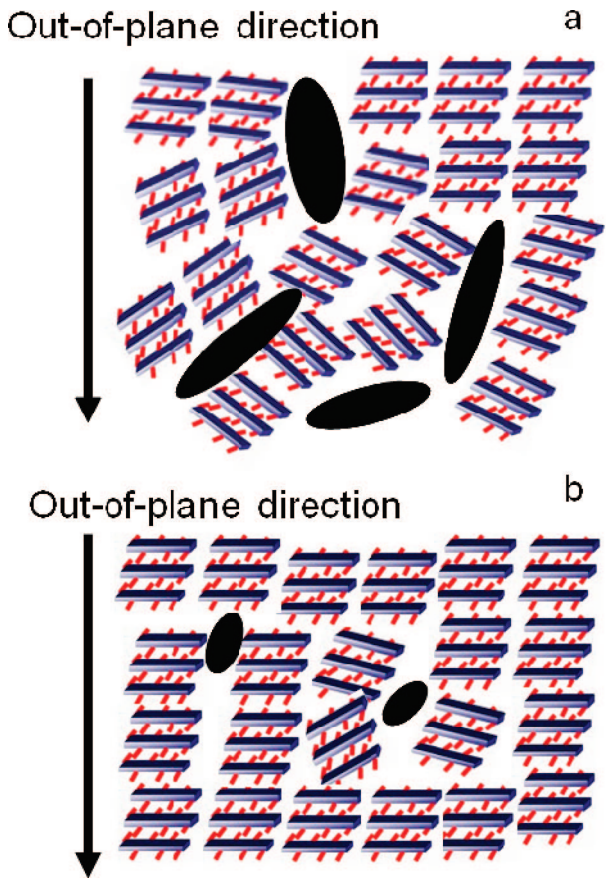

Figure 6. Schematic illustrations of (a) a high-RR P3HT−PCBM blend film containing many large PCBM crystallites, which cause the P3HT stacks to orient away from the out-of-plane direction, and (b) a low-RR P3HT−PCBM blend film with fewer and smaller PCBM crystallites and more ordered P3HT stacks.

confirmed by the narrower crystalline P3HT peaks in the GIXS patterns.

In view of the effect of crystallization-induced phase segregation, the regioregularity of P3HT should be optimized to maintain good electronic properties and high initial device performance while improving thermal stability. Introducing a controlled amount of disorder to the polymer can lead to better blending with PCBM and more stable active-layer morphology. This suggests that in terms of future designs of polymers for solar cells, instead of trying to obtain the highest crystallinity in order to achieve better electronic properties and higher initial device performance, an alternative strategy should be directed toward the search for a polymer that would have favorable interactions with the acceptor material in order to realize the best and most stable morphology for BHJ solar cells.

Conclusions

We have shown that regioregularity is an important variable that affects polymer crystallinity, blend morphology, and device performance. For pristine polymer films, as used in organic transistors, a more regioregular polymer with higher crystallinity and higher mobility gives rise to a better device because of better charge transport. However, in polymer−fullerene-composite solar cells, considerations that apply to the properties of the pristine polymer are complicated by the addition of another component, where blend morphology becomes an important variable. Although higher-RR P3HT has higher optical density and charge-carrier mobility, its increased degree of crystallinity in fact becomes a disadvantage, as it induces more severe phase segregation with PCBM upon thermal annealing. Although only a few regioregularities were examined in this work, we have demonstrated that high RR is not necessary to achieve high-efficiency solar cells and that using a polymer with a lower RR actually has the benefit of improving the thermal stability of the device. In particular, the 86% RR P3HT sample we synthesized not only has sufficient electronic properties to afford high-efficiency photovoltaic devices but also has the advantage of producing more thermally stable devices as a result of less crystallization-induced phase segregation of PCBM. Evidence from optical and electron microscopy and GIXS supports the hypothesis that highly crystalline 96% RR P3HT blends develop many large PCBM crystals that are detrimental to device performance. Our results emphasize the need to take into account the interaction of the blend components when designing materials for BHJ solar cells. In addition to good optical and electronic properties, a polymer for photovoltaic applications must also blend well with the acceptor material in order to achieve the ideal composite morphology with sufficient thermal stability.

Acknowledgment. The authors acknowledge financial support from the Director, Office of Science, Office of Basic Energy Sciences, Division of Materials Sciences and Engineering, of the U.S. Department of Energy under Contract No. DE-AC02-05CH11231; portions of this work were performed at the Molecular Foundry under the same contract. C.H.W. thanks the Department of Defense for a National Defense Science and Engineering Graduate (NDSEG) Fellowship. B.C.T. thanks the American Chemical Society Petroleum Research Fund for an Alternative Energy Postdoctoral Fellowship. The authors also thank Alex C. Mayer and Michael D. McGehee of the Department of Materials Science and Engineering at Stanford University for assistance with scattering measurements. Portions of this research were carried out at the Stanford Synchrotron Radiation Laboratory, a national user facility operated by Stanford University on behalf of the U.S. Department of Energy, Office of Basic Energy Sciences.

Supporting Information Available: Synthetic details, experimental procedures, polymer characterization, TEM images, SEM images, a schematic illustration of P3HT organization, and DSC scans. This material is available free of charge via the Internet at http://pubs.acs.org.

JA806493N